

PROPAGATION EFFECTS AND THEIR IMPACT ON SATELLITE-EARTH LINKS

BER

Communications system design requires the development of a link budget between the transmitter and the receiver that provides an adequate signal level at the receiver's demodulator to achieve the required level of performance and availability. The performance of a link is usually defined for time percentages in excess of 99% over periods of at least a month and is, for digital systems, determined by the bit error rate (BER) that provides the minimum level of service. For analog systems, the C/N at the demodulator input that provides the minimum signal quality required defines the performance level for that link. The availability of a link is usually defined for low outage time percentages (typically between 0.04 and 0.5% of a year, or between 0.2 and 2.5% of the worst month, for satellite systems) and is, for digital systems, specified by the BER at which an outage is declared for the link. For analog systems, the C/N at the demodulator input at which no usable signal can be demodulated defines the limit of availability. Figure 8.1 illustrates the concept of performance and availability for a digital system with BER as the determinant.

The link budget was covered in Chapter 4, as was link margin: the difference in power level between clear sky conditions (essentially the performance level) and that which exists at the threshold of the demodulator when the link is under impaired conditions (the availability level). Actually, there are two margins to consider in a link budget: (1) the margin between the "clear sky" level and the performance threshold; and (2) the margin between the performance threshold and the availability threshold. Figure 8.2 illustrates these two concepts of margin for a typical digital Ku-band downlink (11 GHz) located in the Mid-Atlantic region of the United States. As can be seen, the attenuation experienced on the link varies with time percentage, gradually falling through the performance threshold and then the availability threshold. It is the link designer's task to ensure that loss of signal occurs for no longer than the time permitted for that service. The development of an accurate link budget, which includes losses due to the passage of the signal through the atmosphere, is therefore critical.

The key equation in the development of the link power budget in Chapter 4 was Eq. (4.11), repeated here in modified form as Eq. (8.1).

$$\Rightarrow P_r = \text{EIRP} + G_r - L_p - L_a \text{ dBW} \quad (8.1)$$

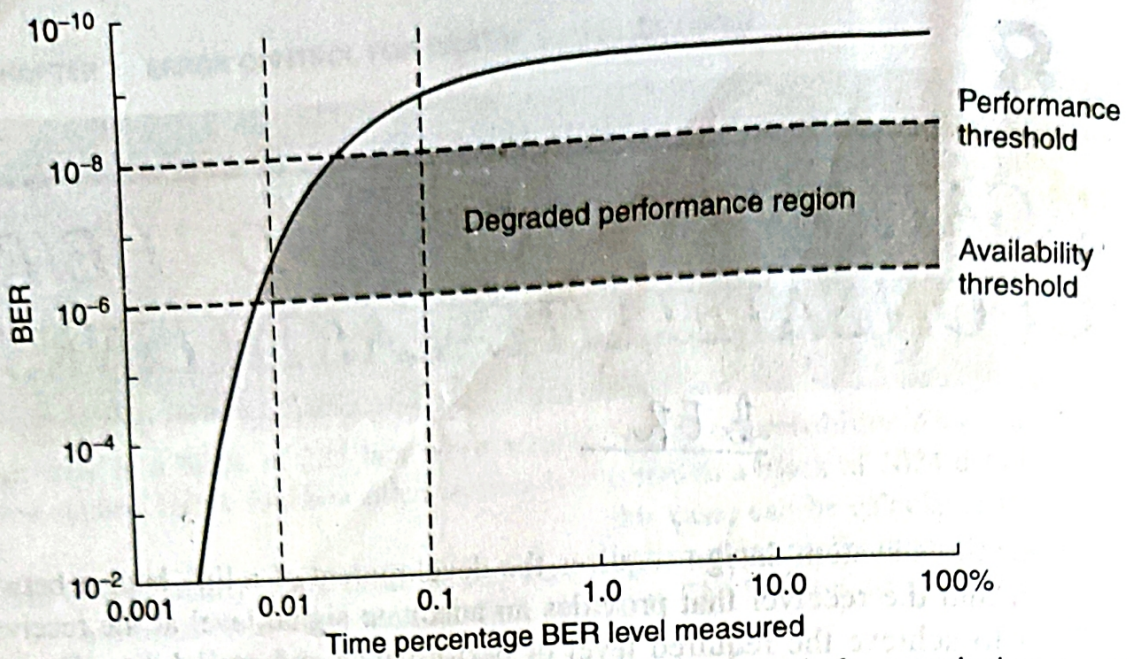


FIGURE 8.1 Schematic of the bit error rate (BER) statistic for a typical communications link. A link is normally designed to provide a given performance specification for a very high percentage of the time. In this example, a BER of 10^{-8} is the performance required for 99.9% of the time. The time period over which the statistics are taken is usually a year or a month. Atmospheric constituents (gases, clouds, rain, etc.) will cause the BER in clear sky condition to degrade. At some point, the BER will reach the level at which an outage is declared. This point defines the availability specification. In this example, a BER of 10^{-6} is the availability threshold and it must be met, in this example, for a minimum of 0.01% of the time.

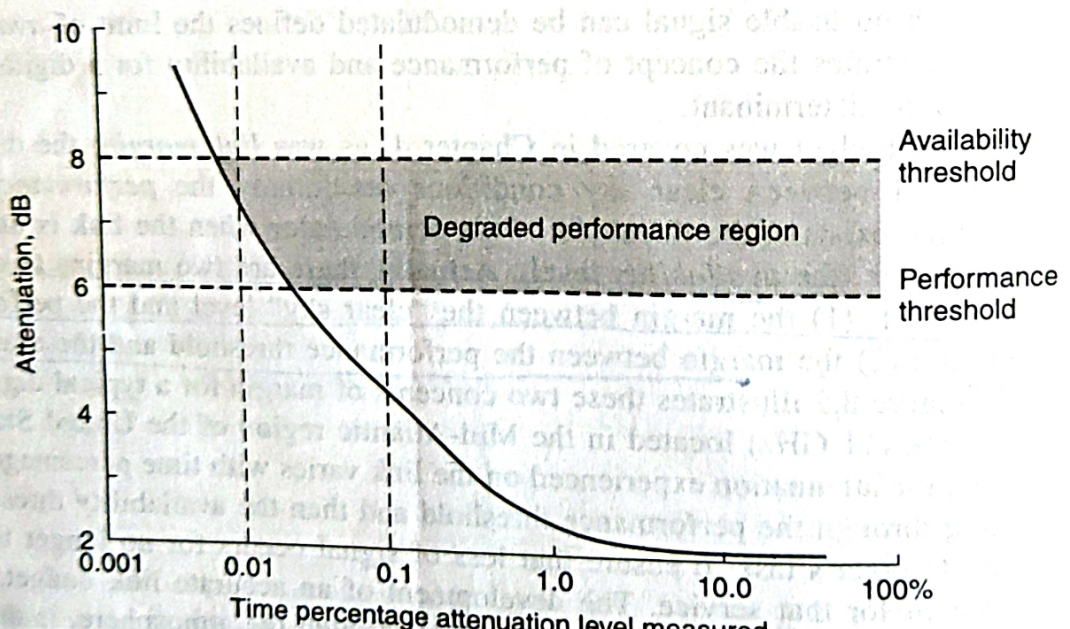


FIGURE 8.2 Schematic of the loss statistics encountered by a signal on transmission through the atmosphere for a typical Ku-band communications link. In most communications links, an allowance in power margin is built into the link so that the received signal is above the threshold for satisfactory demodulation and decoding. This power margin is commonly referred to as the *fade margin* since the signal, on occasion, appears to fade below the level established in clear sky conditions. In the schematic above, the link experiences an equivalent fade of about 1 dB before it reaches the performance threshold level established for the link (see Figure 8.1). A further fade of 2 dB, making a total reduction in signal level of 8 dB, takes the link below the availability level established for the link (see Figure 8.1). The relationship between power level, fade margin, and BER, will depend on the modulation used. It will also depend on the amount of channel coding used. In the example above, no inner (FEC) or outer (Reed-Solomon, interleaved) coding has been assumed for the link and the modulation is QPSK. For most heavily coded links, the difference between good performance and an outage (a change on the order of 2 to 3 decades of BER) will occur for a change in signal level of less than 1 dB.

This equation indicates how the received power, P_r , in dBW depends on the transmitter EIRP (the Effective Isotropic Radiated Power, which is a combination of the output amplifier power, the gain of the transmitting antenna, and the losses associated with that antenna system), the receiving antenna gain, G_r (which includes, in this case, all losses associated with the receiving antenna), the path loss, L_p , (given by $20 \log_{10} [4\pi R/\lambda]$, with λ being the wavelength of the signal and R the distance between the transmitting antenna and the receiving antenna) and the attenuation contribution due to the atmosphere, L_a . Of the terms on the right hand side of equation (8.1), the only one that is not essentially constant with time is the atmospheric loss, L_a . The component L_a , usually referred to as propagation loss, determines the margin required by the communications link to meet both the performance and availability specifications.

1 INTRODUCTION

There are many phenomena that lead to signal loss on transmission through the earth's atmosphere. These include: Atmospheric Absorption (gaseous effects); Cloud Attenuation (aerosol and ice particle effects); Tropospheric Scintillation (refractive effects); Faraday Rotation (an ionospheric effect); Ionospheric Scintillation (a second ionospheric effect); Rain Attenuation; and Rain and Ice Crystal Depolarization. Rain attenuation is by far the most important of these losses for frequencies above 10 GHz, because it can cause the largest attenuation and is usually, therefore, the limiting factor in Ku and Ka band satellite link design. Raindrops absorb and scatter electromagnetic waves. In Ku and Ka bands, rain attenuation is almost entirely caused by absorption. At Ka band, there is a small contribution from scattering by large raindrops. The various propagation loss mechanisms are illustrated in Fig. 8.3. We will discuss each of these loss mechanisms briefly; for a detailed treatment the reader should refer to references 1 and 2.

Figures 8.1 and 8.2 introduced the concept of a time varying BER (or excess link attenuation). Fig. 8.3 indicates where each of the loss mechanisms can be found along the slant path to the satellite. It is also very useful to develop an appreciation for the various time percentages over which each of the propagation loss mechanisms is significant. Figure 8.4 illustrates this schematically, using the same curves from Fig. 8.1.

Signal loss—i.e. attenuation—affects all radio systems; those that employ orthogonal polarizations to transmit two different channels on a common, or partially overlapping, frequency band may also experience degradations caused by depolarization. This is the conversion of energy from the wanted (i.e., the co-polarized) channel into the unwanted (i.e., the cross-polarized) channel. Under ideal conditions, depolarization will not occur. When depolarization does occur, it can cause co-channel interference and cross-talk between dual-polarized satellite links. Rain is a primary cause of depolarization.

Both attenuation and depolarization come from interactions between the propagating electromagnetic waves and whatever is in the atmosphere at the time. The atmospheric constituents may include free electrons, ions, neutral atoms, molecules, and hydrometeors (an arcane term that conveniently describes any falling particle in the atmosphere that contains water: raindrops, snowflakes, sleet, hail, ice-crystals, graupel, etc.); many of these come in a wide variety of sizes. Their interaction with radio waves depends strongly on frequency, and effects that dominate 30 GHz propagation, for example, may be negligible at 4 GHz. The converse is also true. With one major exception (ionospheric effects) almost all propagation effects become more severe as the frequency increases.

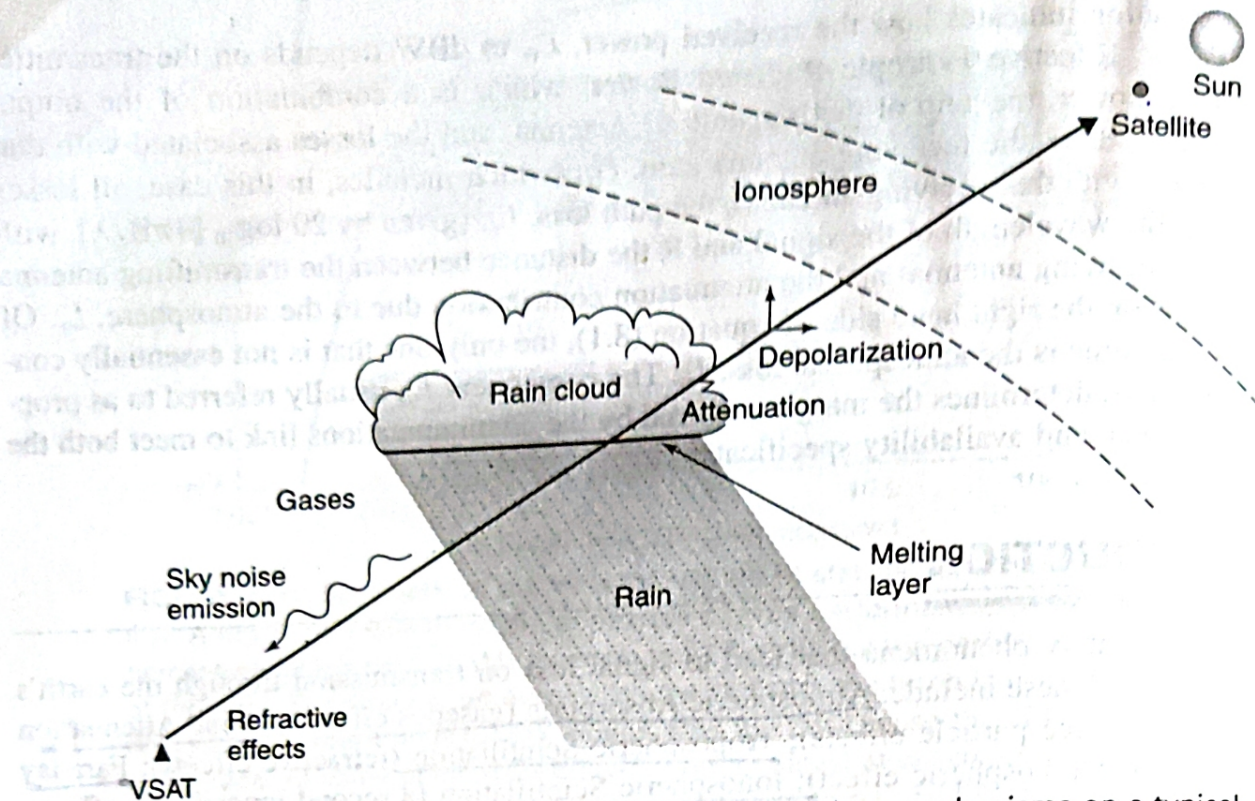


FIGURE 8.3 Illustration of the various propagation loss mechanisms on a typical earth-space path. The earth terminal (in this example a very small aperture terminal or VSAT) is directed toward a satellite. Refractive effects (causing tropospheric scintillation); gases; a rain cloud, melting layer, and rain, all exist in the path and cause signal loss. The absorptive effects of the atmospheric constituents cause an increase in sky noise to be observed by the VSAT receiver. While atmospheric gases and tropospheric scintillation do not cause signal depolarization, collections of nonsymmetrical ice crystals and rain particles can depolarize the transmissions through them. Above the lower (neutral) atmosphere is the ionosphere, which begins at about 40 km and extends well above 600 km. The ionosphere can cause the electric vector of signals passing through it to rotate away from their original polarization direction, hence causing signal depolarization. At certain times of the day, year, and 11-year sunspot cycle, the ionosphere can cause the amplitude and phase of signals passing through it to change rapidly, i.e., to scintillate, about a general mean level. The ionosphere has its principal impact on signals at frequencies well below 10 GHz while the other effects noted in the figure above become increasingly strong as the frequency of the signal goes above 10 GHz. Finally, if the sun (a very "hot" microwave and millimeter wave source of incoherent energy) is in the VSAT beam, an increased noise contribution results which may cause the C/N to drop below the demodulator threshold. Note: The above picture is not drawn to scale. Most rainstorms occur below 10 km altitude and the ionosphere is not normally present below 40 km, and extends to more than 1000 km above the earth.

8.2 QUANTIFYING ATTENUATION AND DEPOLARIZATION

Attenuation, A , is the decibel difference between the power received, P_r , at a given time t and the power received under ideal propagation conditions (often referred to as "clear sky" conditions). With all values in decibel units, we have

$$\rightarrow A(t) = P_{r_{\text{clearsky}}} - P_r(t) \quad (8.2)$$

Attenuation, $A(t)$, on satellite communications links operating at C, Ku, and Ka-band is primarily caused by absorption of the signal in rain. On most satellite links above 10 GHz,

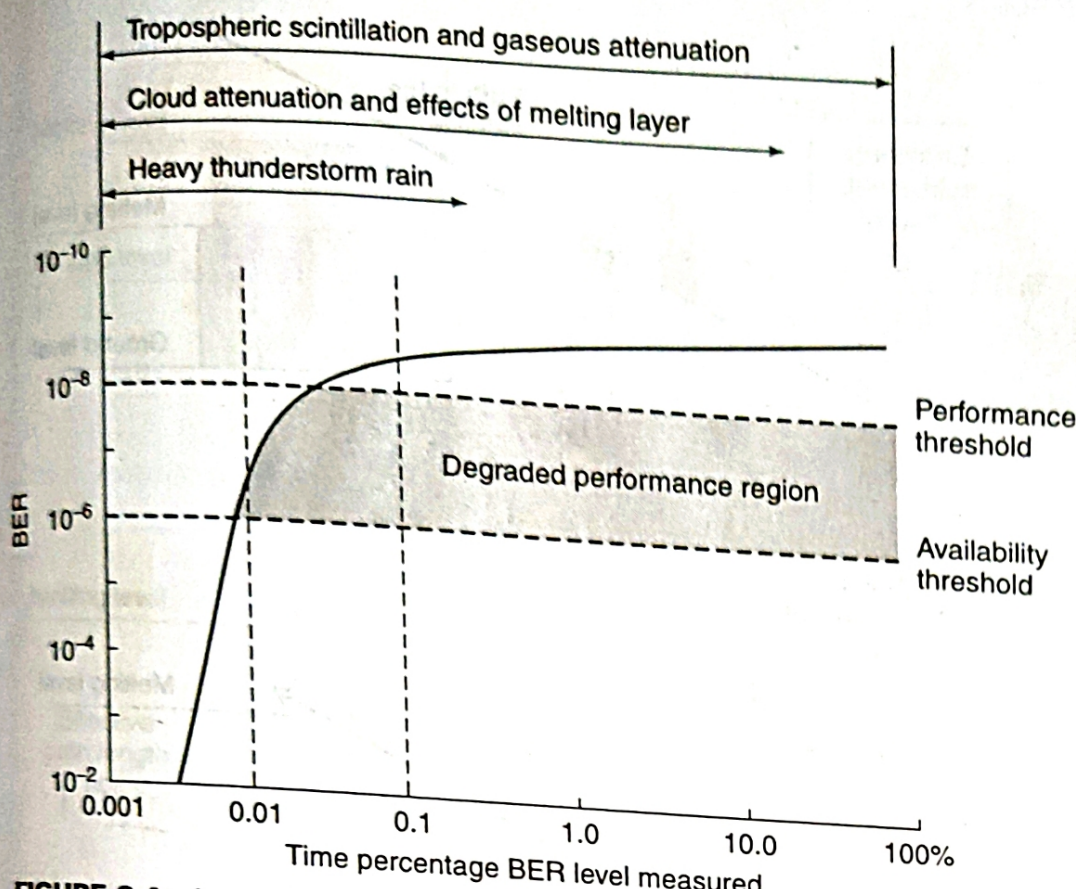


FIGURE 8.4 Approximate range of annual time percentages that various atmospheric im-

pairments affect a link (after Figure 2 of reference 3 © John Wiley & Sons, Inc. Reprinted with permission). Tropospheric scintillation (a refractive effect in the lower atmosphere) and gaseous attenuation are pervasive phenomena that occur all of the time, but at different levels of impact depending on the climate, elevation angle, and time percentage of interest. Clouds exist at various time percentages, depending on the climate, but are generally present for at least 30% of the time in most locations. As the concentration of the frozen particles in the cloud increases, many will start to fall and will melt on reaching the 0°C isotherm. This will lead to enhanced attenuation in the melting layer. Drizzle rain will fall when the water vapor concentration reaches saturation levels. Such rain is usually stratiform and falls for between 1 and 10% of the time, depending on the climate. During hot periods, convective rain will fall, often in the form of thunderstorms. Heavy thunderstorms account for the highest rainfall rates, and hence the highest path attenuations encountered, but they exist for only small time percentages in a year. Not shown in the above figure are ionospheric effects, which have a diurnal, seasonal, and 11-year cyclical impact, again depending on where the earth station is and the precise earth-space path used.

rain attenuation limits the availability of the system and, to develop an adequate link margin, the rain attenuation to be expected for a given time percentage needs to be calculated. This can be a complicated process, but there are basically three steps: (a) determine the rainfall rate for the time percentage of interest; (b) calculate the specific attenuation of the signal at this rainfall rate in dB/km; and (c) find the effective length of the path over which this specific attenuation applies. The difficult part of this process is part (c) because rain falls in two broad categories: stratiform rain and convective rain. These two separate atmospheric mechanisms have different effects on satellite paths. Stratiform rain is generated in cloud layers containing ice, and results in widespread rain or snow at rainfall rates of less than 10 mm per hour. Convective rain is generated by vertical air currents that can be very powerful, leading to thunderstorms and high rainfall rates. Convective rain is very important for satellite communication systems because it is the major cause

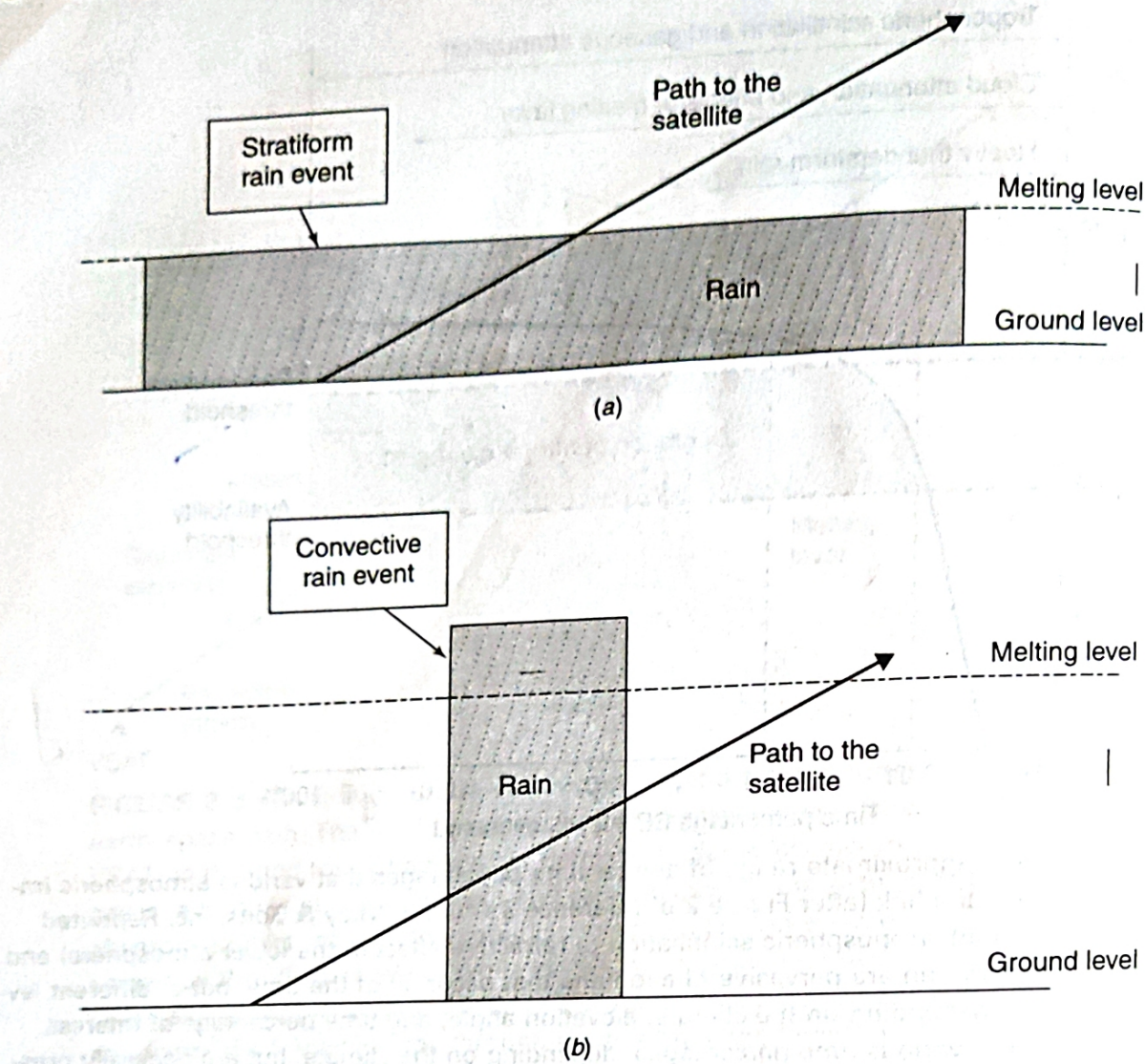


FIGURE 8.5 (a) Stratiform rain situation. In this case, a widespread system of stratiform rain—that is rain that appears to be stratified horizontally—completely covers the path to the satellite from the ground up to the point where the rain temperature is 0°C . This level is called the melting level because, above it, the precipitation is frozen and consists of snow and ice crystal particles. Frozen precipitation causes negligible attenuation. In general, the signal path in stratiform rain will exit the rain through the top of the rain structure. (b) Convective rain situation. In this case, a tall column of convective rain enters the satellite-to-ground path. In some cases the storm will be in front of the earth station; in others, behind it. Convective storms normally occur in the summer, thus the melting level is much higher than in winter. In many cases, the melting level is not well defined, as the strong convective activity inside the storm will push the liquid rain well above the melting level height. Except for paths with very high elevation angles ($>70^{\circ}$), the signal path in convective rain will most often exit from the side of a convective rainstorm.

of link outages. Stratiform rain consists of a generally constant rainfall rate over a very large area while convective rain is generally confined to a narrow, but tall, column of rain. Figure 8.5 illustrates the two rain processes and Figure 8.6 gives the concept of the path attenuation calculation procedure for both rain types.

Stratiform rain occurs typically ahead of a warm front in an area of low pressure. Large areas of cloud exist in which ice crystals are sufficiently large to slowly fall and join other ice crystals to form snowflakes, which fall more quickly as their size increases. If there is a high concentration of moisture in the clouds, in the form of ice, large snowflakes may form. The snow falls until it reaches the *melting layer*. The melting layer is simply the region of the atmosphere where the temperature transitions from below 0°C

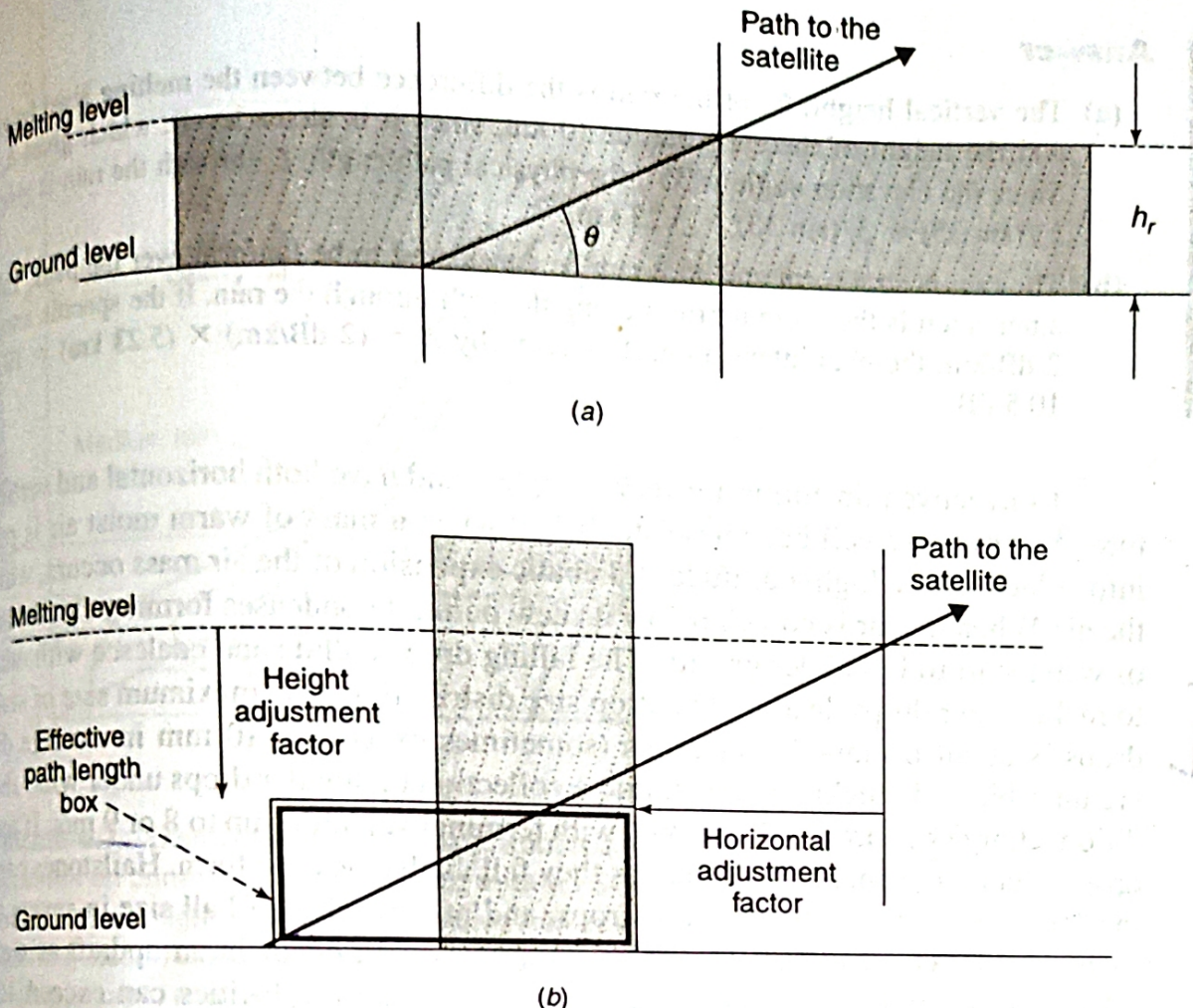


FIGURE 8.6 (a) Stratiform rain attenuation calculation procedure. In the case of stratiform rain, the rainfall rate along the path can be considered to be uniform and the path completely immersed in the rain. The effective path through the rain—the path over which the rain may be considered to be uniform—is therefore the same as the physical path length in stratiform rain. The path attenuation A is therefore the specific attenuation (i.e., dB attenuation per km) multiplied by the physical path length in the rain (i.e., $h_r/\sin \theta$). (b) Convective rain attenuation calculation procedure. In the case of convective rain, the melting level and elevation angle are used to develop two adjustment factors: a height adjustment factor and a horizontal adjustment factor. Once these factors have been used, a smaller box is created inside which it may be assumed that the rainfall rate is uniform. The length of the path that exists inside this box is the effective path length and it is this that is used to multiply the specific attenuation with. In this case, the path exits through the top of the effective path length box. In other cases, it may exit through the side.

to above 0°C . Snow falling into air at a temperature greater than 0°C melts and forms raindrops. If the air at the earth's surface is below 0°C the snow does not melt, but continues to the ground. The stratiform cloud mechanisms that generate snow result in low rainfall rates, always less than 10 mm per hour, and widespread (stratiform) rain or snow. This leads to generally constant attenuation of the slant-path signals over the entire path length from the ground to the melting layer.

EXAMPLE 8.2.1

An earth station at sea level communicates at an elevation angle of 35° with a GEO satellite. The melting level height of the stratiform rain is 3 km. Find (a) the physical pathlength through the rain; (b) find the path attenuation if the specific attenuation is 0.1 dB/km .

Answer

- (a) The vertical height, h_r , of the rain is the difference between the melting level height (3 km) and the height of the earth station (0 km, since it is at sea level), which gives $h_r = 3 \text{ km}$. Since the elevation angle is 35° , the physical pathlength, L , through the rain is given by $L = h_r / (\sin 35^\circ) = 3 / (\sin 35^\circ) = 5.23 \text{ km}$.
- (b) The rain is stratiform and so it can be considered to be uniform over the path. The specific attenuation is therefore uniform along the path through the rain. If the specific attenuation is 2 dB/km, the path attenuation, A is given by $A = (2 \text{ dB/km}) \times (5.23 \text{ km}) = 10.46 \text{ dB} \approx 10.5 \text{ dB}$

Convective rainstorms are very complex, and have both horizontal and vertical structure. A convective cell becomes established when a mass of warm moist air is pushed up into colder air at a higher altitude. Adiabatic expansion of the air mass occurs, which cools the air. When the air is cooled below its dew point, it condenses forming clouds, and drops of water start to fall under gravity. The falling drops collide and coalesce with other drops to make larger drops, leading to a drop size distribution. The maximum size of stable raindrops is about 6 mm—larger drops (sometimes exceeding 10 mm in average diameter) are unstable and quickly break up into a collection of smaller drops under wind shear conditions. Large raindrops fall quickly, with terminal velocities up to 8 or 9 m/s. If the falling drops encounter supercooled water as they fall, hailstones can form. Hailstones can exceed the 10+ mm diameter limit of raindrops, and may reach golf ball size in severe thunderstorms in the Great Plains. The accretion process can occur in an updraft as well as for falling drops, and in a vigorous thunderstorm, updraft velocities can exceed 100 mph. Since cold air is denser than warm air, once an updraft dies away at the top of a thunderstorm, cold air tends to flow downward, and can create a streamer, a narrow region of intense rain and cold air. Streamers can be a few hundred meters wide or a kilometer wide. At the surface, the streamer is observed as a microburst, which has strong wind shear as the vertical down flow of cold air hits the ground and spills out in all directions. We are all familiar with microbursts. Shortly before heavy rain falls there is often a cold wind, followed by a downpour. The cold wind we feel is the outflow of cold air as it hits the earth's surface. The effect of convective rain on a satellite slant path depends on the angle at which the path intersects a streamer. Streamers are rarely vertical, so if a slant path

SIDE BAR

Microbursts are dangerous for aircraft flying close to the ground, especially when taking off and landing. Several serious accidents to passenger aircraft in the 1980s were attributed to the wind shear associated with microbursts, and extensive research was carried out to develop ways to detect microbursts and wind shear. Networks of anemometers, which measure wind speed, can be deployed around an airfield to detect wind shear, and terminal Doppler radar can be used for the same purpose.

An aircraft on final approach to a runway is flying slowly and descending on a 3° glide slope. If the aircraft encounters a microburst, it first experiences a headwind, which increases its speed relative to the air

and tends to slow the rate of descent. The natural reaction of the pilot is to reduce engine power to maintain a constant rate of descent on the 3° glide slope. However, as soon as the aircraft passes the center of the microburst, the wind direction is opposite, and is now a tailwind, which reduces the speed of the aircraft relative to the air and increases the rate of descent of the aircraft. If the engine power has been cut, the airplane may sink into the ground before the engines have developed enough power to keep the airplane aloft. Wind shear detection equipment at airfields and improved pilot awareness of the dangers of microbursts have reduced the incidence of accidents caused by microbursts.

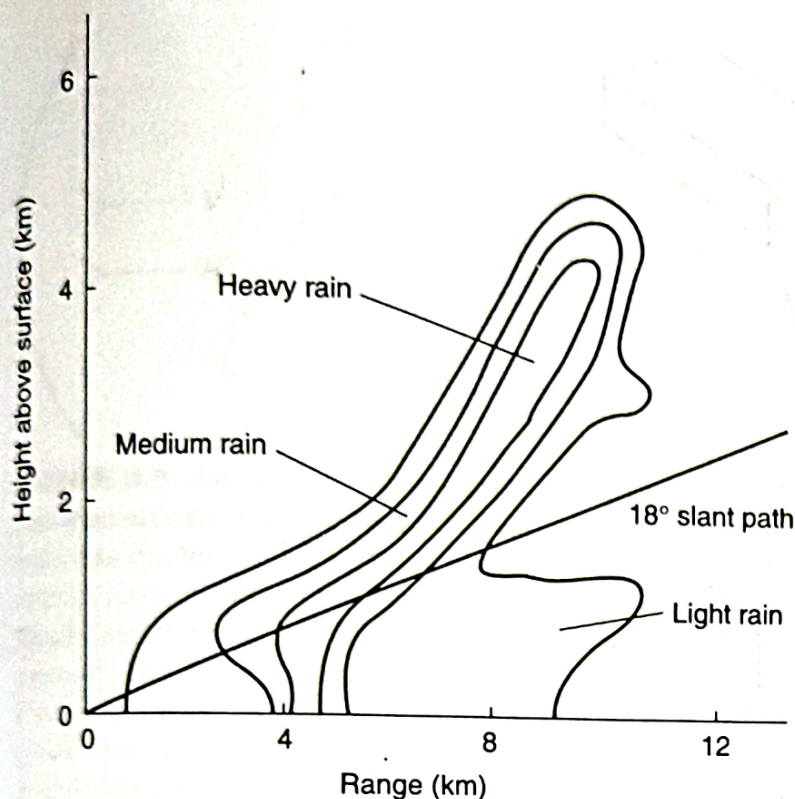


FIGURE 8.7 Example of an RHI scan through a rain storm. Radar reflectivity contours in a rainstorm on June 15, 1986, measured with an S-band radar in Blacksburg, Virginia. The contours represent light, medium, and heavy rain in a narrow vertical column. The radar and a receiving station were collocated at the (0,0) point. Note the narrow extent of heavy rain in a sloping column, and the effect on the slant path to the satellite at an elevation angle of 18°. The statistical rain height H_r for Blacksburg is 4.1 km. In this example, rain is present up to an altitude of 5.6 km above sea level.

is parallel to a streamer it will suffer very heavy attenuation if the streamer envelops the path. If the slant path cuts across the streamer, the path length within the heavy rain may be quite short, leading to relatively little attenuation despite the high rainfall rate.

Figure 8.7 shows an example of a convective rain cell observed with an S-band radar at Virginia Tech's satellite tracking station. The radar was used to make vertical scans across the slant path to a satellite (known to radar people as an *RHI scan*, for range-height indicator, a WWII radar display mode). The complex shape of the storm cell requires the use of artificial "adjustment factors" to convert the physical path through the rainstorm to an effective path length over which the rain may be considered to be uniform. As well as causing significant attenuation, rain and ice crystals can cause depolarization.

Depolarization is more difficult to quantify than attenuation. All signals have a polarization orientation that is defined by the electric field vector of the signal. (See Figure 8.8.) In general, signals are never purely polarized; the direction of the electric field will never be perfectly oriented or constant. Successful orthogonal polarization frequency sharing—usually called dual-polarization frequency reuse—requires that there be sufficient isolation between two orthogonal polarization states to permit the separation of the wanted polarization (the copolarized signal) from the unwanted polarization (the cross-polarized signal) at the receiving antenna.⁵ The difference between the copolarized and the cross-polarized signal energy will determine the cross-polarization discrimination at the receiver, the XPD, and hence the level of interference between two orthogonally polarized signals.

To illustrate the process by which depolarization is measured; imagine a dual-polarized antenna transmitting orthogonally polarized signals. We will call the two polarizations *V* (for vertical) and *H* (for horizontal) for convenience, although there

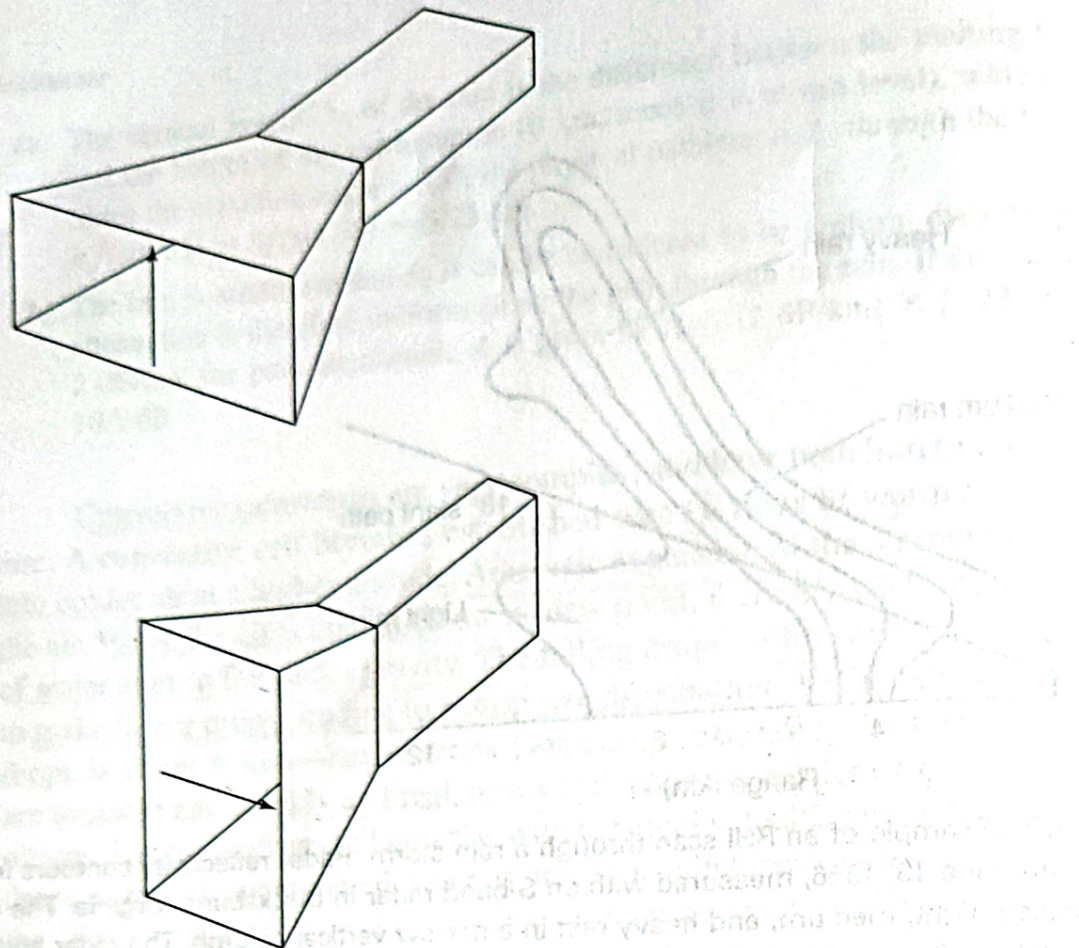


FIGURE 8.8 Orthogonally polarized waveguide horn antennas. The polarization of an electromagnetic wave is defined by the orientation of the electric vector. In the example above, two waveguide horns, excited in the TE_{10} mode, are radiating in the same direction. The top horn is oriented such that the electric vector is vertically polarized; the bottom horn is turned on its side compared with the top horn and so the electric vector is horizontally polarized. The arrows indicate the electric field vector. Since the electric polarization vectors are oriented 90° with respect to each other in the two horns, the transmitted signals are considered to be orthogonally polarized. Orthogonally polarized signals do not interfere with each other, even if they are at exactly the same frequency, provided they are "purely" polarized (i.e., there is no component of the signal present in the other, orthogonal, polarization). In all cases, however, the transmitted signals are not purely polarized, due to antenna imperfections, so a component exists in the unwanted polarization. In addition, some of the energy in one polarization can "cross" over to the other polarization due to asymmetric particles (e.g., large, oblate raindrops) existing in the propagation path. This cross-polarized energy can give rise to interference between the two, mutually orthogonal polarizations. The degree of cross-polarization to be expected along a given path is predicted using cross-polarization models that are usually based on the rain attenuation along the path.

are infinitely many orthogonal polarization pairs. Let the complex phasor amplitudes of the transmitted electric field vectors with polarization V and H be \mathbf{a} and \mathbf{b} , respectively, as shown in Figure 8.9. The transmitting antenna is excited so that \mathbf{a} and \mathbf{b} are equal.

If the transmission medium between the transmitting and receiving antennas were clear air, phasor \mathbf{a} would give rise to a V polarization wave of amplitude a_c at the receiving antenna and phasor \mathbf{b} would cause an H polarization wave of amplitude b_c . The subscript c stands for copolarized; these fields have the same polarization sense as their transmitted counterparts. (See Figure 8.10.)

If asymmetrical rain or ice crystal particles exist in the transmission medium, some of the energy in \mathbf{a} will couple into a small (cross-polarized) H polarized field component.

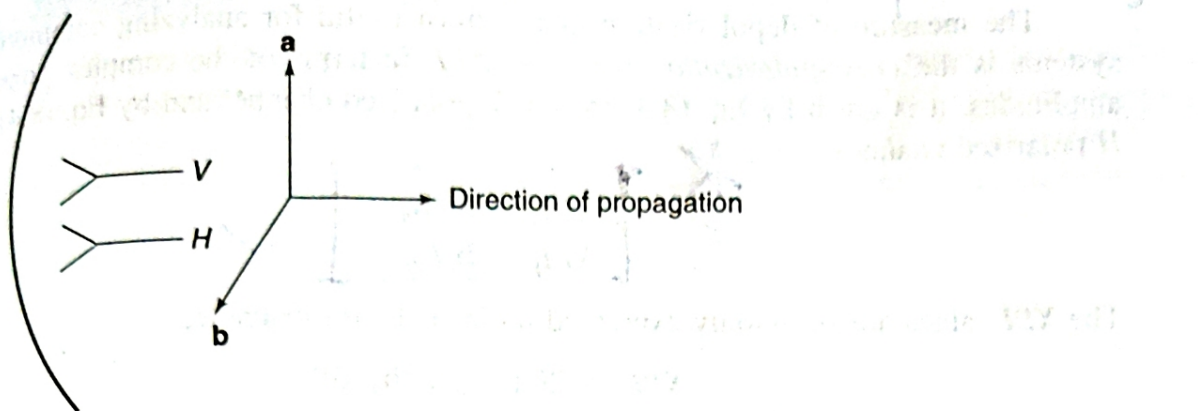


FIGURE 8.9 Fields excited by a dual-polarized antenna. The field radiated by the *V* horn has the vertically polarized electric field vector indicated by **a** and the field radiated by the *H* horn has the horizontally polarized field vector indicated by **b**. In most antenna systems, one horn is used to radiate both polarizations simultaneously rather than two. This permits the single feed horn to be located at the prime focus of the antenna to generate the best far field pattern⁵. The two polarization senses to be transmitted are excited in separate parts of the transmitter and are then coupled together via an ortho-mode transducer into a single waveguide section. This waveguide section, which can support both polarizations simultaneously, is then used to couple the signals into a waveguide horn that is capable of radiating both polarizations senses equally.

whose amplitude at the receiving antenna is \mathbf{a}_x , and \mathbf{b} will give rise to a small (cross-polarized) *V* polarized component \mathbf{b}_x . An ideal receiving system that introduces no cross-polarization will have a *V* channel output ($\mathbf{a}_c + \mathbf{b}_x$) and an *H* channel output ($\mathbf{b}_c + \mathbf{a}_x$). The unwanted \mathbf{b}_x term represents interference with the wanted signal \mathbf{a}_c and the unwanted \mathbf{a}_x term is interference with the wanted signal \mathbf{b}_c . This interference will cause cross talk on an analog link and increase the BER on a digital link. This generation of unwanted cross-polarized components is called depolarization.

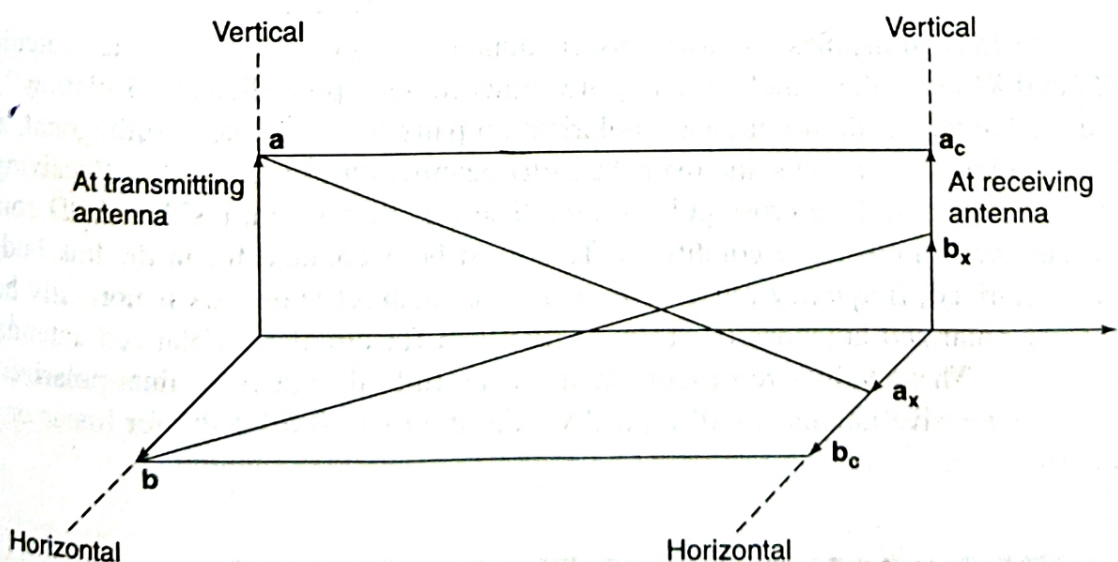


FIGURE 8.10 Illustration of signal depolarization in the transmission path. The transmitted fields **a** and **b** produce copolarized components \mathbf{a}_c and \mathbf{b}_c at the receiving antenna. The transmission medium in this instance is not clear sky, nor is the transmitting antenna perfectly polarized, and the anisotropy of the transmission medium and imperfections in the transmitting antenna induce cross-polarized components of the transmitted signal to be received. These cross-polarized components at the receiving antenna are \mathbf{a}_x and \mathbf{b}_x . With perfect antennas and in the absence of depolarization \mathbf{a}_x and \mathbf{b}_x would be zero.

~~cross polarisation~~ ~~discrimination~~

The measure of depolarization that is most useful for analyzing communications systems is the cross-polarization isolation, XPI. In terms of the complex phasor field amplitudes, it is given by Eq. (8.3) for the V polarized channel and by Eq. (8.4) for the H polarized channel.

$$\cancel{XPI_V = \frac{a_c}{b_x}} \quad (8.3)$$

$$XPI_H = \frac{b_c}{a_x} \quad (8.4)$$

The XPI values are commonly expressed in decibels; for example,

$$XPI_V = 20 \log_{10} |a_c/b_x| \text{ dB} \quad (8.5)$$

Physically, the XPI is the decibel ratio of wanted power to unwanted power in the same channel. The larger the XPI value, the less interference there is and the better the communications channel will perform. XPI is difficult to measure. It requires the simultaneous transmission of signals at the same frequency in both polarization senses. The COMSTAR series of satellites had a beacon that rapidly switched between two orthogonal polarization senses, thus permitting the measurement of XPI [e.g., 6, 7]. More recently, the ACTS⁸ and OLYMPUS⁹ satellites also incorporated a switched beacon to permit XPI measurements. Most propagation experiments are much simpler than this and measure simultaneously the wanted (the copolarized) and the orthogonal, unwanted (the cross-polarized) signals that are received from a satellite beacon that transmits in only one polarization. In this case (referring to Figure 8.10) the experiment would measure (say) signals a_c and a_x that are derived from a singly polarized signal a that is transmitted from the satellite. Measuring received signals b_c and b_x simultaneously from a singly polarized signal b would provide the same result. This process allows the cross-polarization discrimination, XPD to be derived

$$\cancel{XPD_V = a_c/a_x} \quad (8.6)$$

or in decibels

$$XPD_V = 20 \log_{10} |a_c/a_x| \text{ dB} \quad (8.7)$$

In most transmission situations encountered in practice, the values calculated for XPI and XPD are the same¹⁰ and they are sometimes simply called the "isolation." In practice, real antennas do not transmit polarization pairs that are exactly orthogonal, nor does the isolation remain the same over the 3-dB beamwidth of the antenna. Receiving antennas can also introduce cross-polarization. There is therefore a residual XPD component present even in clear sky conditions. This must be accounted for in the link budget of a dual-polarized, frequency reuse system. The residual XPD on axis is normally better for linearly polarized antennas (~30 to 35 dB) than for circularly polarized antennas (~27 to 30 dB). These values represent antennas carefully designed for dual-polarized operation; inexpensive antennas will typically exhibit about 20 dB XPD for linear or circular polarizations.

8.3 PROPAGATION EFFECTS THAT ARE NOT ASSOCIATED WITH HYDROMETEORS

In this section we will discuss propagation effects that are not associated with raindrops or ice crystals: atmospheric absorption, cloud attenuation, refractive effects that include tropospheric scintillation and low angle scattering, multipath effects, Faraday rotation, and ionospheric scintillation.

Atmospheric Absorption

At microwave frequencies and above, electromagnetic waves interact with molecules in the atmosphere to cause signal attenuation. At certain frequencies, resonant absorption occurs and severe attenuation can result. Figure 8.11 (from Figure 6 of reference 11) shows these resonant absorption peaks on a zenith path (that is, a path at an elevation angle of

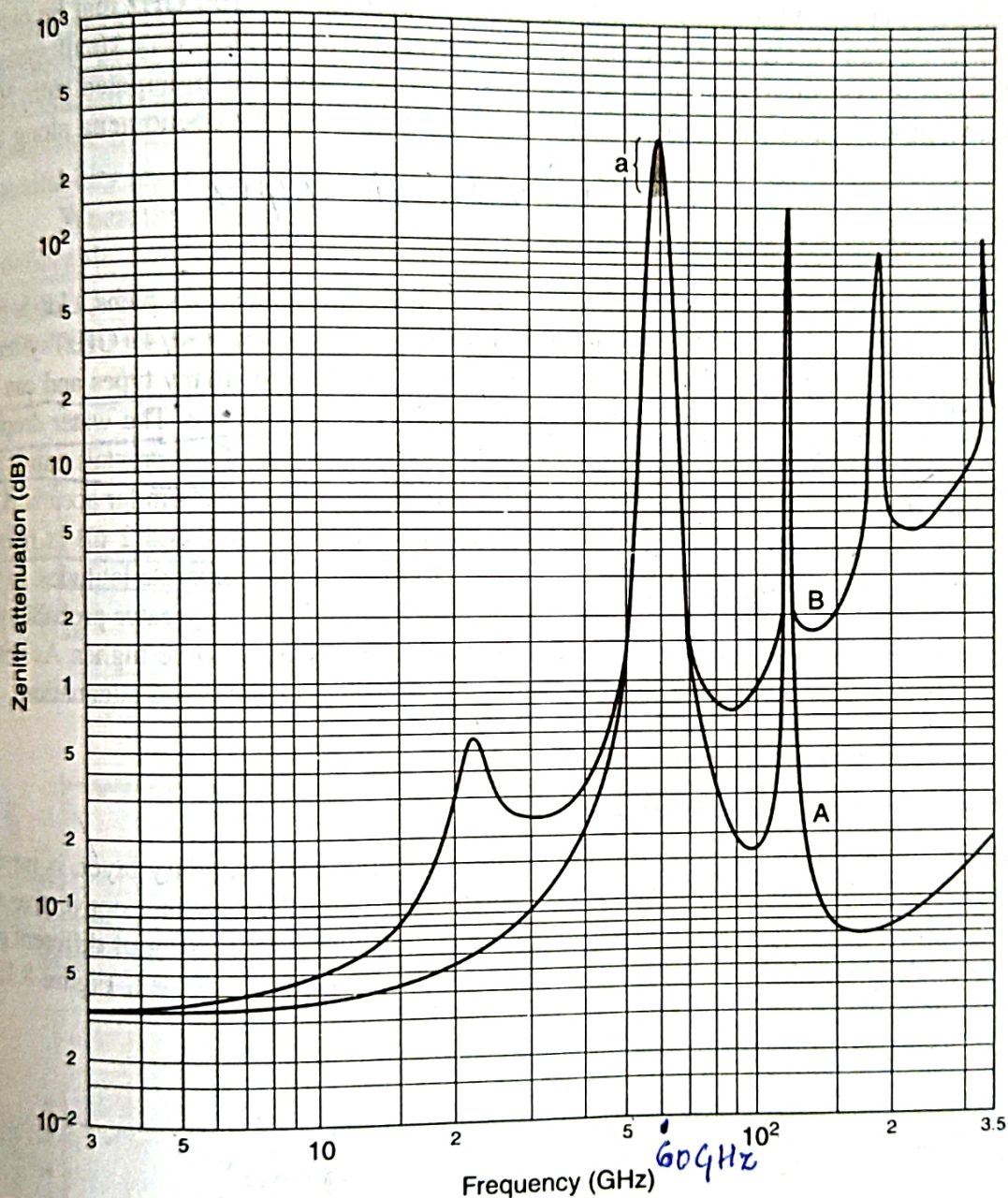


FIGURE 8.11 Total zenith attenuation due to atmospheric gases calculated from 3 to 350 GHz (from Figure 6 of reference 11 © ITU, reproduced with permission). The two curves represent the gaseous attenuation that would be observed looking straight up from sea level (i.e., on a zenith path) right through the neutral atmosphere on a satellite-earth path. Curve A is for a dry atmosphere (i.e., no water vapor present) while curve B is for a standard atmosphere. A standard atmosphere consists of a surface pressure of 1013 hPa [a hPa has the same numerical value as the old pressure unit of millibars], a surface temperature of 15°C, and a surface relative humidity of 7.5 mg/m³. Curve A shows only the resonant absorption peaks of the oxygen molecules (a broad peak at 60 GHz and a narrow peak at 118.75 GHz). Curve B includes the resonant absorption peaks due to the water vapor molecule at 22.235, 183.31, and 325.153 GHz. The shaded portion "a" indicates a range of values since there are many individual resonant absorption lines in this region.

90°) from a sea level location right through the neutral atmosphere. *Neutral* means that no ionization is present.

The first absorption band in Figure 8.11 is that due to water vapor at 22.235 GHz. The K-band sets of frequencies are on both sides of this absorption band, which has led to the terminology of Ku band (signifying frequencies under the absorption band) and Ka band (signifying frequencies above the absorption band). It is common to specify a satellite frequency band by the uplink frequency. From Figure 8.11, it can be seen that gaseous absorption accounts for less than 1 dB on most paths below 100 GHz that lie outside the absorption bands. However, in many new systems that employ very small system margins, it is important to account for the gaseous losses along the anticipated path. New prediction procedures that attempt to account for all attenuating phenomena along the path (e.g., [12]) include gaseous absorption.

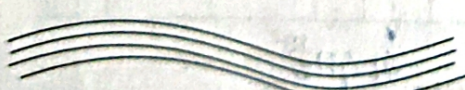
$\hookrightarrow 1-2 \text{ dB } @ 30 \text{ GHz}$

Cloud Attenuation

Once considered to be largely irrelevant for satellite communications paths, clouds have become an important factor for some Ka-Band paths and all V-Band (50/40 GHz) systems. The difficulty with modeling cloud attenuation is that clouds are of many types and can exist at many levels, each type having a different probability of occurrence. The water droplet concentrations in each cloud will also vary, and clouds made up of ice crystals cause little attenuation. Two models have been proposed^{13,14}, both of which have similar accuracy. Typical values of cloud attenuation for water-filled clouds are between 1 and 2 dB at frequencies around 30 GHz on paths at elevation angles of close to 30° in temperate latitudes. In warmer climates, where clouds are generally thicker in extent and have a greater probability of occurrence than temperate latitudes, cloud attenuation is expected to be higher. As with most propagation effects, the lower the elevation angle, the higher the cloud attenuation.

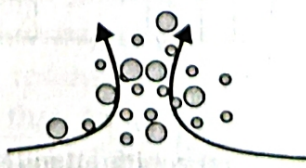
Tropospheric Scintillation and Low Angle Fading

The atmosphere close to the ground, sometimes called the boundary layer, is rarely still. Energy from the sun warms the surface of the earth and the resultant convective activity agitates the boundary layer. This agitation results in turbulent mixing of different parts of the boundary layer, causing small-scale variations in refractive index. Figure 8.12 illustrates the process.



Stratified Layers (calm conditions)

(a)



Turbulent Mixing (convective conditions)

(b)

FIGURE 8.12 Schematic of stratified and turbulent conditions in the boundary layer of the atmosphere. In (a), the air is calm and the lower atmosphere next to the earth's surface (the boundary layer) forms into layers. Each layer has a slightly different refractive index, decreasing in general with height. In (b), the earth's surface has become heated by energy from the sun and the resultant convective activity has mixed the formerly stratified layers into "bubbles" that have different refractive indices. The turbulent mixing in (b) will cause relatively rapid fluctuations in a signal passing through it, which are called scintillations.

Scanned By Scanner

When a signal encounters a turbulent atmosphere, the rapid variation in refractive index along the path will lead to fluctuations in the received signal level. These fluctuations are generally about a fairly constant mean signal level and are called scintillations. Because the bulk of the fluctuations are caused within 4 km of the earth's surface, they are referred to as tropospheric scintillations. Tropospheric scintillations occur in many weather conditions, as can be seen in Figure 8.13.

Tropospheric scintillation does not cause depolarization. The magnitude of the scintillations becomes generally larger as the frequency increases, the path elevation angle reduces, and the climate becomes warmer and more humid. Prediction models exist to calculate this phenomenon with good accuracy¹⁵. On paths below 10° elevation angle, tropospheric scintillation can be performance limiting; below 5° elevation angle it can become availability limiting.

When the elevation angle falls below 10°, a second propagation effect becomes noticeable: low angle fading. Low angle fading is the same phenomenon as multipath fading on terrestrial paths. A signal transmitted from a satellite arrives at the earth station receiving antenna via different paths with different phase shifts. On combination,

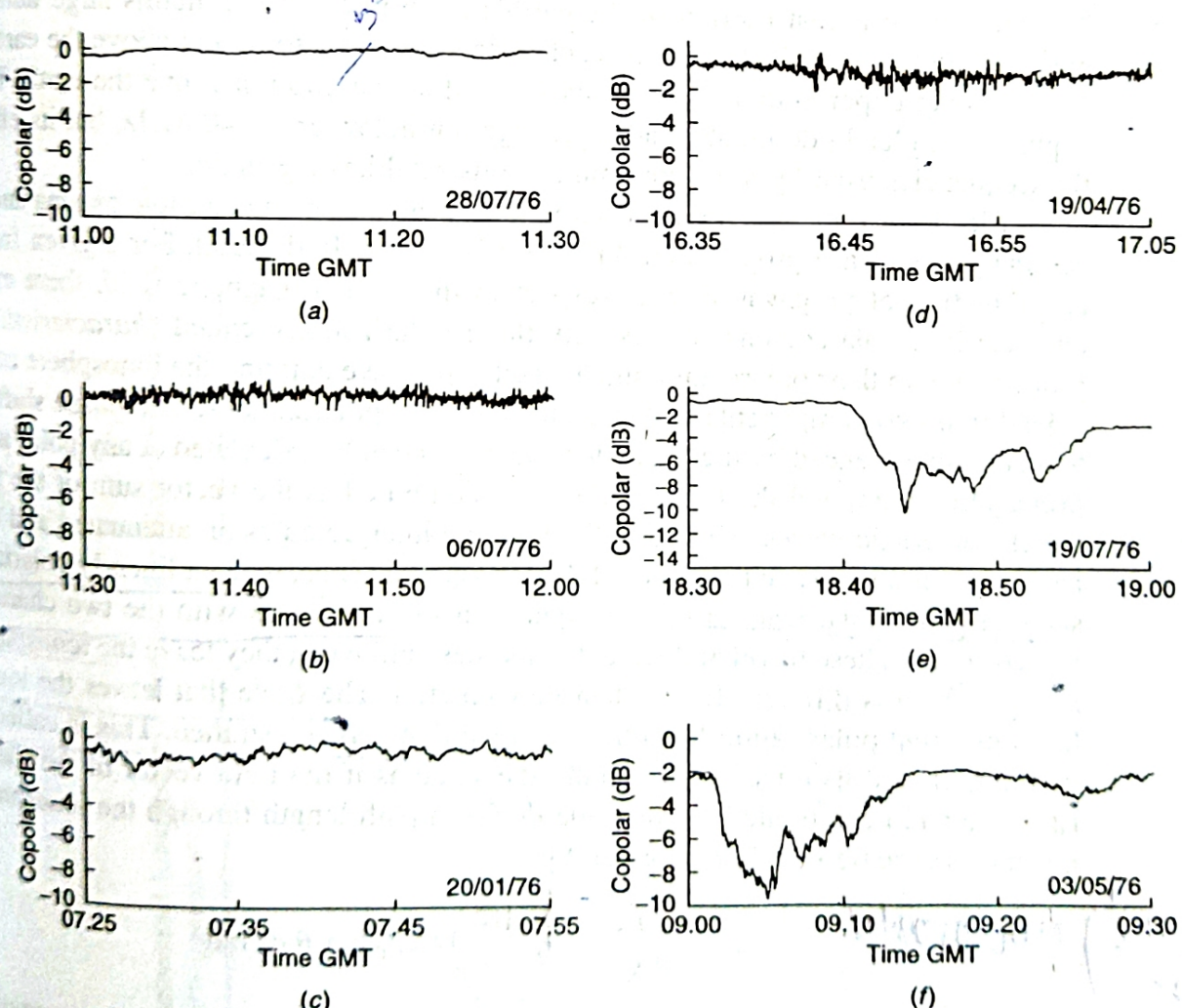


FIGURE 8.13 Scintillations observed under a variety of weather conditions on a 30-GHz downlink from ATS-6 (from reference 16). Scintillations with various amplitudes can be observed under different weather conditions. Two of the data sets were taken in clear weather, two in cloud conditions, and two during rain, as follows: (a) clear-weather copolar signal with low scintillation; (b) clear-weather copolar signal with high scintillation; (c) copolar scintillation in cloud; (d) copolar scintillation in cloud; (e) copolar scintillation and attenuation in rain; (f) copolar scintillation and attenuation in rain. Note the difference in scintillation amplitude under what are apparently similar weather conditions along the path.

the resultant waveform may be enhanced or attenuated from the normal clear sky level. Signal enhancement has been observed to exceed 8 dB on a 3.3° path at 11.198 GHz¹⁷, while cancellation can cause complete link dropout. The mechanism for low angle fading has been interpreted as atmospheric multipath and also as the "defocusing and focusing" of the incoming signal. Both explanations have merit: the received signal is made up of components that have arrived via different paths (i.e., multipath), but the mechanism for developing the different paths is one of refraction rather than reflection at the atmospheric layer boundaries. Low angle fading is only significant in very still air on very low elevation angle paths. It is normally not considered for satellite paths when the elevation angle is above 10°. Note that the multipath effect referred to here is occurring in the atmosphere, and is therefore different from multipath effects in terrestrial radio links which are caused by reflections from the ground, buildings, trees, etc.

Faraday Rotation in the Atmosphere

The ionosphere is that portion of the earth's atmosphere that contains large numbers of electrons and ions. At its lowest, it reaches down to close to 40 km above the earth; there is no distinct upper boundary, but it exists well above 600 km above the earth. The ionosphere completely dominates radio propagation below about 40 MHz, but its effects on the frequencies used by most communications satellites are minor.

Electrically, the ionosphere is an inhomogeneous and anisotropic plasma and an exact analysis of wave propagation through it is extremely difficult. For a given frequency and direction of propagation with respect to the earth's magnetic field, there exist two characteristic polarizations. Waves with these polarizations, called *characteristic waves*, propagate with their polarization unchanged. Any wave entering the ionosphere can be resolved into two components with the characteristic polarizations. The phase shift and attenuation experienced by the characteristic waves can be calculated at any point along the propagation path, and the total field can be computed as the vector sum of the fields of the characteristic waves. This total field can be interpreted as an attenuated and depolarized version of the wave that entered the ionosphere. Thus, when a linearly polarized (LP) satellite path signal reaches the ionosphere, it excites waves with the two characteristic polarizations. These travel at different velocities, and when they leave the ionosphere their relative phase is different from when they entered. The wave that leaves the ionosphere has a different polarization from the LP wave that was transmitted. This is called *Faraday rotation*, and its effect is essentially the same as if the field vector of the transmitted LP wave had been rotated by an angle ϕ . For a path length through the ionosphere of Z meters, the rotation angle ϕ is given by

$$\phi = \int \left(\frac{2.36 \times 10^4}{f^2} \right) Z N B_0 \cos \theta dz \text{ rad} \quad (8.8)$$

Here, θ is the angle between the geomagnetic field and the direction of propagation, N is the electron density in electrons/cubic meter, B_0 is the geomagnetic flux density in Teslas, and f is the operating frequency in Hz. The rotation angle ϕ varies inversely with f^2 . Table 8.1 gives the value of ϕ and some other parameters with frequency¹⁵. The polarizations of an earth station antenna can be adjusted to compensate for the Faraday rotation observed under average conditions. However, the rotation of the uplink will be in an opposite sense to that on the downlink and so it will be necessary to rotate the directions at the same time, a feed will be required that is able to rotate the relevant sections in opposite

directions. The *XPD* that results when the polarization angle of an LP wave changes by an amount $\Delta\phi$ is given by

$$XPD = 20 \log_{10}(\cot \Delta\phi) \quad (8.9)$$

Hence, a 6° change from average conditions would reduce the *XPD* on the link to about 19.6 dB.

Ionospheric Scintillations

Energy from the sun causes the ionosphere to "grow" during the day, increasing the total electron content (TEC) by two orders of magnitude, or more. The TEC is the total number of electrons that would exist in a vertical column of area 1 m^2 from the surface of the earth all the way through the earth's atmosphere. Typical values of TEC range from $\sim 10^{12}$ during the day to $\sim 10^{16}$ during the night. It is the rapid change in TEC from the daytime value to the nighttime value, which occurs at local sunset in the ionosphere, that gives rise to irregularities in the ionosphere. The irregularities cause the signal to vary rapidly in amplitude and phase, which leads to rapid signal fluctuations that are called *ionospheric scintillations*. The magnitude of the ionospheric scintillations varies with time of day, month in the year, and year in the 11-year sunspot cycle. The greatest scintillation effects are observed just after local sunset in the equinox periods during the sunspot maximum years. The effects are also worst within about $\pm 20^\circ$ of the geomagnetic equator and over the poles. The length of the cycles averages at around 11 years, but has been as short as 9.5 years and as long as 12.5^{18} . Solar sunspot cycle 22 was from 1986.8 to 1996.4.

8.4 RAIN AND ICE EFFECTS

At frequencies above 10 GHz, rain is the dominant propagation phenomenon on satellite links. Many experiments have been conducted on geostationary satellite links, using experimental satellites such as SIRIO, OTS, and CTS (Hermes) at Ku Band and ATS-6, OLYMPUS, and ACTS at Ka Band. One experimental satellite, Italsat, also allowed 50/40 GHz (V Band) experiments to be conducted in Europe. References 1, 2, 8, and 9 provide detailed results and explanations of all the propagation phenomena.

Characterizing Rain

Most farmers, hydrologists, and city planners need to know how much total rain will fall in a given period: that is, the *rain accumulation*. Indeed, most weather forecasts are given in terms of how much precipitation will fall (or accumulate) over a given region. Rain accumulation, unfortunately, is of little use to satellite link designers, since it is the rate at which the rain is falling that is important: that is, the *rainfall rate*. Rainfall rate is measured by a rain gauge, the most common of which is a tipping bucket rain gauge. This is fairly accurate between rainfall rates of 10 to 100 mm/h. Peak values of 100 to 150 mm/h may be expected for short periods during summer thunderstorms in the mid-Atlantic region of the United States. Higher rainfall rates are observed in tropical regions.

The long-term behavior of rainfall rate is described by a *cumulative probability distribution* or by a *cumulative distribution function (cdf)*. The cdf for rainfall rate is commonly referred to as an *exceedance curve*. This gives the percentage of time (usually the percentage of 1 year) that the rainfall rate exceeds a given value. Climate related parameters tend to be very variable. Rain accumulation can vary significantly from year-to-year.

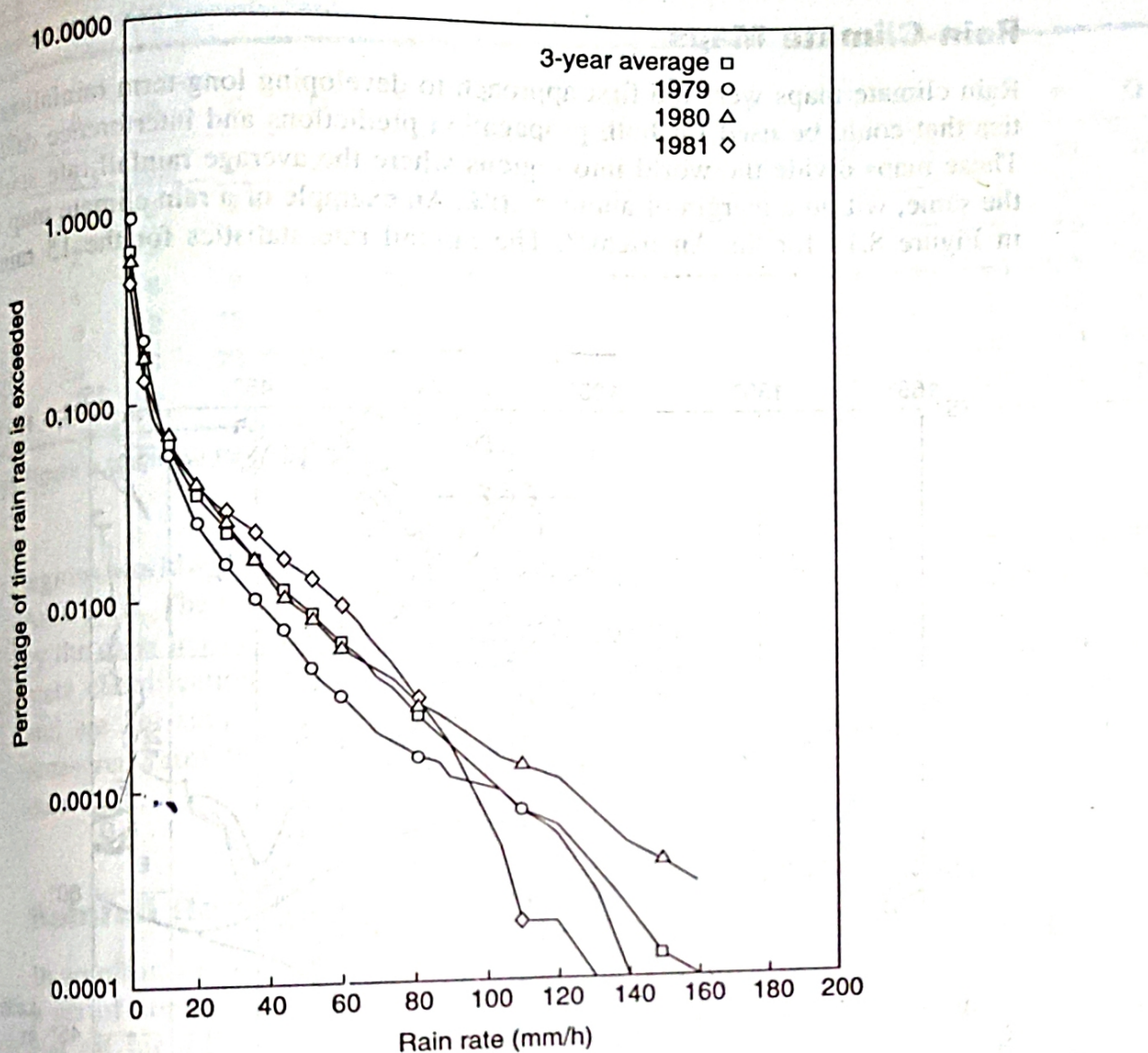


FIGURE 8.14 Typical rainfall rate cumulative probability distributions or "exceedance" curves. These sets were measured at Virginia Tech, Blacksburg, United States as part of a 3-year experiment with the Italian satellite, SIRIO. The 1979 data indicate a relatively dry year, while those of 1981 indicate a relatively wet year. Despite this, a single, rare thunderstorm in 1979 produced much higher rainfall rates than those observed in 1981 at low time percentages. The availability level the link has to operate at will determine what rainfall rate is of most importance and it will also give a range over which the design must cope. For example, if 0.01% was the availability requirement, in 1979 the rainfall rate for this time percentage was 38 mm/h while in 1981 it was 58 mm/h. This shows the value of long-term statistics so that one year's data do not bias the link design.

as can the exceedance curves, particularly at the low time percentages of interest to satellite link designers.

Three annual exceedance curves taken from an experiment performed at Blacksburg, Virginia, are shown in Figure 8.14 and it can be seen that the rainfall rate at the 0.01% point varies between 38 and 58 mm/h over the 3 years. The cumulative attenuation curves for the 3 years showed similar trends. Depending on the elevation angle of the link, this can make a significant difference in the attenuation measured at the same time percentage in each of the years. For this reason, link designers prefer to use values averaged over many years of measurements for their propagation models. There have been two approaches to developing these long-term statistics: rain climate maps and exceedance contour maps.

Rain Climate Maps

Rain climate maps were the first approach to developing long-term rainfall rate statistics that could be used for both propagation predictions and interference calculations. These maps divide the world into regions where the average rainfall rate statistics are the same, within a margin of about $\pm 10\%$. An example of a rain climate map is shown in Figure 8.15 for the Americas¹⁹. The rainfall rate statistics for the 15 rain climate

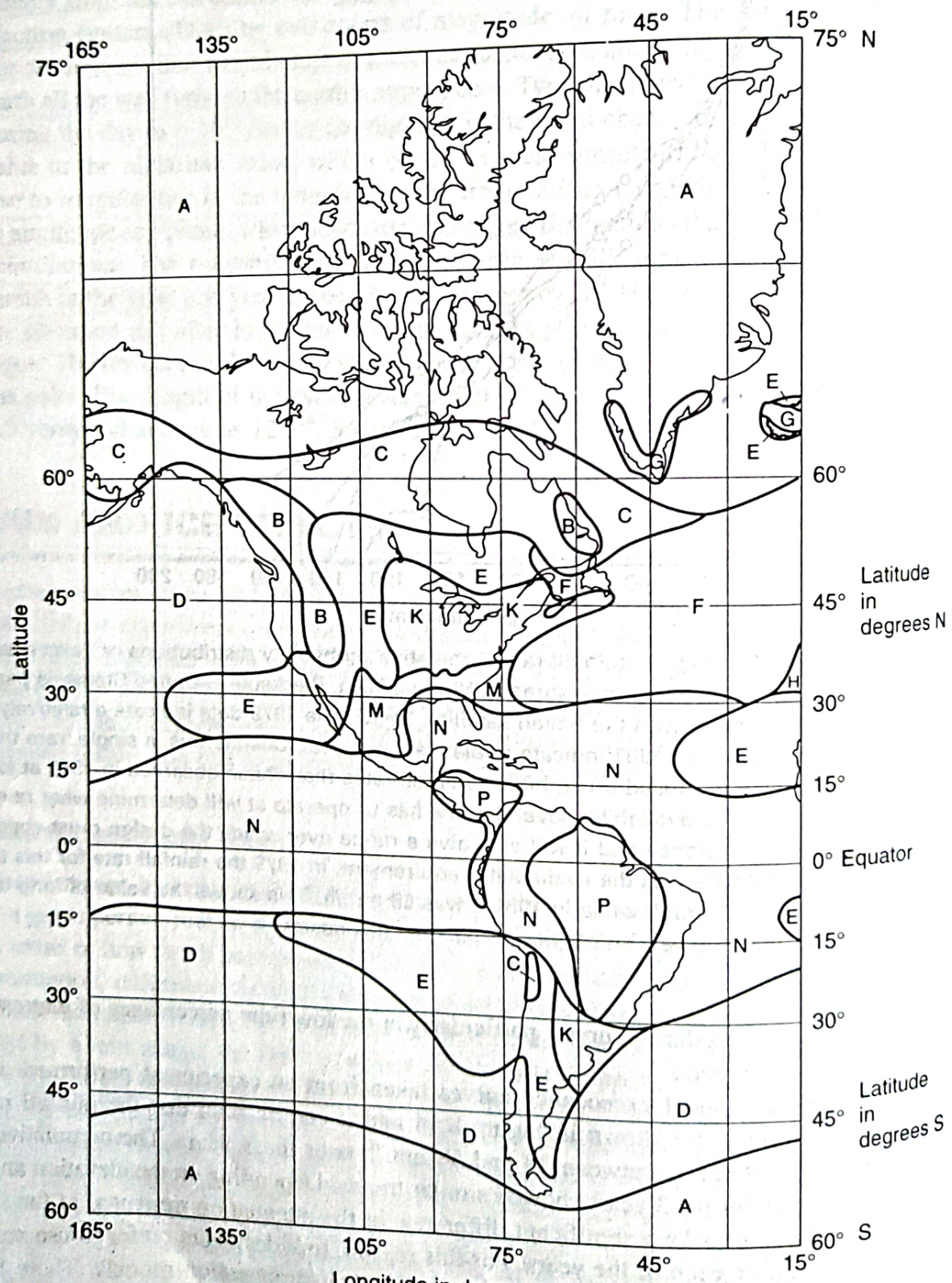


FIGURE 8.15 Rain climatic zones for the Americas (Scanned By Scanner Go reproduced with permission). (from Figure 1 of reference 19 © ITU)

TABLE 8.2 Rainfall Rate Intensities for the Rain Climatic Zones (From TABLE 1 in [19] © ITU, reproduced with permission)

Percentage of Time (%)	A	B	C	D	E	F	G	H	J	K	L	M	N	P	Q
10	<0.1	0.5	0.7	2.1	0.6	1.7	3	2	8	1.5	2	4	5	12	24
0.3	0.8	2	2.8	4.5	2.4	4.5	7	4	13	4.2	7	11	15	34	49
0.1	2	3	5	8	6	8	12	10	20	12	15	22	35	65	72
0.03	5	6	9	13	12	15	20	18	28	23	33	40	65	105	96
0.01	8	12	15	19	22	28	30	32	35	42	60	63	95	145	115
0.003	14	21	26	29	41	54	45	55	45	70	105	95	140	200	142
0.001	22	32	42	42	70	78	65	83	55	100	150	120	180	250	170

NOTE: See Figure 8.12 for the Rain Climatic Zones in N. and S. America

regions worldwide are given in Table 8.2. (Note that not all of these regions exist in the Americas). The ease with which the tables and rain climate maps can be used is offset by the clear inaccuracies that occur when large parts of the earth are given the same climate classification. The step-changes across the climate boundaries are also arbitrary and are not supported by measured data. Wherever possible, it is always best to use measured rainfall rate data as the attenuation prediction model input whenever these data exist.

Rainfall Rate Exceedance Contour Maps

In an effort to overcome the inaccuracies of the rain climate maps, the ITU developed a set of comprehensive rainfall rate exceedance curves for the whole world. An initial set for the Americas is shown in Figure 8.16. These maps are updated periodically and the latest set can be found on the ITU web site²⁰. An example is shown in Figure 8.17²².

Raindrop Distributions

Rain attenuation and depolarization occur because individual raindrops absorb energy from radio waves. The drops absorb some of the incident energy and some is scattered. The size and shape of raindrops have been measured². The most common mathematical description of the distribution of raindrop sizes is exponential and of the form

$$N(D) = N_0 e^{(-D/D_m)} \text{ mm}^{-1} \text{ m}^{-3} \quad (8.10)$$

where D_m is the median drop diameter and $N(D)$ dD is the number of drops per cubic meter with diameters between D and $D + dD$ mm. The rainfall rate R is related to $N(D)$ and also to the terminal velocity $V(D)$ of the falling drops in meters per second with diameter D by²³

$$R = 0.6 \times 10^{-3} \pi \int D^3 V(D) N(D) dD \text{ mm/h} \quad (8.11)$$

The details of scattering and absorption by a single raindrop, and the summation over the drop population that the calculation of path attenuation from the drop size distribution requires are beyond the scope of this text.